Characteristics of Bio-Oil-Syngas and Its Utilization in Fischer−Tropsch Synthesis

Zhao Xiang Wang,[†] Ting Dong,[†] Li Xia Yuan,[†] Tao Kan,[†] Xi Feng Zhu,[†] Youshifumi Torimoto,[‡] Masayoshi Sadakata,[§] and Quan Xin Li*,[†]

Department of Chemical Physics, Lab of Biomass Clean Energy, University of Science & Technology of China, Hefei, Anhui, 230026, P.R. China, Oxy Japan Corporation, 7# Floor, Miya Building, 4-3-4, Kojimachi, Chiyoda-ku, Tokyo 102-0083, Japan, and Department of Environmental Chemical Engineering, Kogakuin University, 2665-1, Nakano-machi Hachioji-shi, Tokyo 192-0015, Japan

Received January 19, 2007. Revised Manuscript Received April 30, 2007

The Fischer−Tropsch synthesis (FTS) using bio-oil-syngas has been investigated as a potential approach to obtaining clean liquid bio-fuels. Bio-oil-syngas, defined as the syngas obtained from bio-oil steam reforming, was generated via the catalytic steam reforming of homemade bio-oil. Bio-oil reforming performances including the hydrogen yield, carbon conversion, and main composition of the bio-oil-syngas have been investigated over three different catalysts (C12A7/15%Mg, 12%Ni/γ-Al_2O_3, and 1%Pt/γ-Al_2O_3) in a fixed-bed flow reactor. It was found that the most important parameters for steam reforming of the bio-oil were the temperature, the molar ratio of steam to carbon fed (S/C), and the reforming catalyst types. H_2 and CO_2 were the major reforming products together with a small amount of CO and CH_4 in the effluent gaseous products of bio-oil steam reforming. The new catalyst C12A7/15%Mg exhibited high reforming activity under the optimum steam reforming conditions. The hydrogen yield of about 71% with a carbon conversion over 93% was obtained over the C12A7/15%Mg catalyst under reforming conditions of $T = 750$ °C, S/C = 6.0, and gas hourly space velocity (GHSV) = 26 000 h^{-1}. Furthermore, FTS was performed in a fixed-bed flow reactor by using the $H_2/CO/CO_2/N_2$ mixture as a model bio-oil-syngas. The effects of temperature (T), total pressure (P), contact time (W/F), and the $CO_2/(CO + CO_2)$ ratio (r) on the FTS performance were investigated over the coprecipitated iron catalyst of Fe/Cu/Al/K. To obtain a higher total carbon ($CO + CO_2$) conversion and higher C_{5+} selectivity, it was found that the optimum FTS conditions over the Fe/Cu/Al/K catalyst are $T = 280\sim300$ °C, $P = 1.0\sim2.0$ MPa, and $W/F > 12.5$ g_{cat}•h•mol^{-1}. A total carbon ($CO + CO_2$) conversion of about 36% and a C_{5+} selectivity of about 44% were obtained under typical reaction conditions: $T = 300$ °C, $P = 1.5$ MPa, and $W/F = 12.5$ g_{cat}•h•mol^{-1}. It was also found that the $CO_2/(CO + CO_2)$ ratio of the syngas has a remarkable effect on FTS performance, and $r < 0.5$ is more suitable for FTS in our investigated range. The characteristics of steam reforming catalysts and the FTS catalyst were also investigated by various characterization measurements.

1. Introduction

Concerns about the depletion of fossil fuel reserves and the pollution caused by continuously increasing energy demands make biomass an attractive alternative energy source. Biomass is regarded as a renewable hydrocarbon resource, which is photosynthesized from water and carbon dioxide by plants. In the case that biomass is utilized to as an energy resource, the emission of carbon dioxide caused by its use is absorbed by newly grown biomass, and this is called being carbon-neutral. Biomass can offer the possibility to produce liquid, carbon-neutral transportation fuels. Ethanol, methanol, and synthetic hydrocarbons, as well as hydrogen, can be produced from biomass and could offer feasible alternatives for the transport sector on foreseeable terms.[1] In addition, for the negligible sulfur, nitrogen, and metal contents compared with fossil fuels, biomass is a clean energy source. The use of biomass as an energy resource has received much attention recently, because of its ability to provide additional energy and, at the same time, reduce greenhouse gas emissions. As with any energy resource, there are limitations on the use and applicability of biomass, and it must compete not only with fossil fuels but with other renewable energy sources such as wind, solar, and wave power.[2] According to the Energy Information Administration Web site (http://www.eia.doe.gov/fuelrenewable.html), biomass only accounts for less than 3% of the total energy use in the U.S.A. However, it should be noted that technological developments [in conversion, as well as long-distance biomass supply chains (i.e., comprising intercontinental transport of biomass-derived energy carriers)], can dramatically improve the competitiveness and efficiency of bioenergy.[3]

Up to now, various technologies, for example, pyrolysis of biomass,[4,5] biomass gasification,[6,7] and biochemical methods,[2] have been explored to utilize biomass energy. It is well-known

* Corresponding author. Tel.: +86-551-3601118. Fax: +86-551-3606689. E-mail: liqx@ustc.edu.cn.
[†] University of Science & Technology of China.
[‡] Oxy Japan Corporation.
[§] Kogakuin University.

(1) Faaij, A. P. C.; Hamelinck, C. N.; Tijmensen, M. *Proceedings of the First World Conference on Biomass for Energy and Industry*; James & James Ltd.: London, U.K., 2001; Vol. 1/2, pp 687−690.
(2) McKendry, P. *Bioresour. Technol.* **2002**, *83*, 47−54.
(3) Faaij, A. *Mitigation Adapt. Strat. Global Change* **2006**, *11*, 343−375.
(4) Bridgwater, A. V. *Catal. Today* **1996**, *29*, 285−295.
(5) Garcia, L.; Salvador, M. L.; Arauzo, J.; Bilbao, R. *J. Anal. Appl. Pyrolysis* **2001**, *58−59*, 491−501.
(6) Aznar, M. P.; Caballero, M. A.; Corella, J.; Molina, G.; Toledo, J. M. *Energy Fuels* **2006**, *20*, 1305−1309.

10.1021/ef0700275 CCC: $37.00
Published on Web 06/05/2007

that bio-oil is mainly generated from biomass via a fast pyrolysis process,[8,9] which generally contains numerous oxygenated organic compounds including acids, alcohols, aldehydes, ketones, substituted phenolics, and other complex oxygenates derived from biomass carbohydrates and lignin. From the viewpoint of real application, bio-oil has many advantages such as collection, transportation, and storage. However, the properties of bio-oil also result in several significant problems during its use as fuel in standard equipment such as boilers, engines, and gas turbines constructed for combustion petroleum-derived fuels. Since most bio-oils are polar, viscous, and corrosive and contain 40−50 wt % oxygen, their direct use as conventional fuel would be ruled out. An undesired effect, especially observed when the oils are stored or handled at higher temperatures, is an increase in viscosity with time.[10] This is believed to result from chemical reactions between various compounds present in the oil, leading to the formation of larger molecules. There is also evidence that bio-oil can react with oxygen from air. The bio-oils also polymerize when heated to relatively low temperatures.[11] Probably, it is easier to realize the conversion of bio-oil to liquid bio-fuels on a large scale, in comparison with the direct conversion of biomass. Thus, we are focusing on our target in (1) producing bio-oil by the fast pyrolysis of biomass,[12,13] (2) catalytic steam reforming of bio-oil to produce bio-oil-syngas, and (3) producing clean liquid biofuels by Fischer−Tropsch synthesis (FTS) from bio-oil-syngas.

The compound $12CaO{\cdot}7Al_2O_3$ (C12A7), one of the crystalline phases in the system of CaO and Al_2O_3, is a major constituent in aluminous cements. The microporous material of C12A7 usually is produced by the calcination of $CaCO_3$ and γ-Al_2O_3 powder with a molar ratio of 12:7 under a flowing oxygen atmosphere.[14] The structure of C12A7 is cubic with a lattice constant of 1.1989 nm and is characterized by a positively charged lattice framework $[Ca_{24}Al_{28}O_{64}]^{4+}$ including 12-sub-nanometer-sized cages with a free space of about 0.4 nm in diameter.[15−19] The microporous material of C12A7 can store and emit the oxygen radical anion of O^-.[14,20,21] The concentration of O^- stored in the bulk of C12A7 is about 3.7×10^{20} cm^{-3} by electron paramagnetic resonance measurements.[22,23] On the other hand, the O^- anion stored in the cages can be desorbed into the gas phase by heating the C12A7 material to a certain temperature.[20,21] It is well-known that the active O^- anion is a key intermediate in anion chemistry, particularly in the low-temperature oxidation of hydrocarbons.[24−30] Because C12A7 has unique O^- storage and emission features, this material can be used as an active catalyst to oxygenate or decompose some chemicals (e.g., hydrocarbons etc.).[31−34] For example, it has been reported that C12A7 had good activity for the catalytic pyrolysis of naphtha[35] and for the steam cracking of *n*-hexane to produce ethylene.[32,33] We also observed the oxidation and decomposition of benzene over the C12A7 surface.[34] Some metal-promoted (Ni-, Co-, etc.) C12A7's have been tested as good catalysts for the partial oxidation of methane to produce syngas.[36,37] Potassium-promoted C12A7 has high activity for the steam pyrolysis of *n*-heptane[38−40] and methylcyclohexane.[41] More recently, we found that the C12A7 catalyst was active in the hydroxylation of benzene[34] to produce phenol, and the potassium-doped C12A7 catalyst (C12A7/K) has high activity for NOx storage and reduction.[42] The present work shows that the MgO-doped C12A7 catalyst (C12A7/Mg) has higher activity for the steam reforming of bio-oil.

The FTS reaction, $CO + H_2 =$ hydrocarbons $+ H_2O$, was discovered by Fischer and Tropsch in 1925.[43] It can produce liquid fuels such as gasoline and diesel oil from coal or natural gas. The interest in FTS has been revived in recent years as a consequence of environmental demands and an increase in the known reserves of natural gas. Compared to conventional fuels (gasoline and diesel), FT fuels contain no sulfur and low aromatics. Furthermore, FT fuels may be suitable as a hydrogen source for fuel cell vehicles via on-board reforming, because they are free of fuel cell catalyst poisons (e.g., sulfur). A disadvantage of FT fuels is that they have a very low octane number and need to further increase their octane number by reforming for gasoline use. Some recent studies indicated that the use of FT technology for biomass conversion via biomass gasification to synthetic hydrocarbons may offer a promising

(7) Radmanesh, R.; Chaouki, J.; Guy, C. *AIChE J.* **2006**, *52* (12), 4258−4272.
(8) Czernik, S.; Bridgwater, A. V. *Energy Fuels* **2004**, *18*, 590−598.
(9) Bridgwater, A. V.; Meier, D.; Radlein D. *Org. Geochem.* **1999**, *30*, 1479−1493.
(10) Czernik, S.; Johnson, D.; Black, S. *Biomass Bioenergy* **1994**, *7*, 187−192.
(11) Sharma, R. K.; Bakhshi N. N. *Energy Fuels* **1993**, *7*, 306−314.
(12) Zhu, X. F.; Zheng, J. L.; Guo, Q. X.; Zhu, Q. S. *J. Environ. Sci.* **2006**, *18*, 392−396.
(13) Zhu, X. F.; Venderbosch, R. *Fuel* **2005**, *84*, 1007−1010.
(14) Li, Q. X.; Hayashi, K.; Nishioka, M.; Kashiwagi, H.; Hirano, M.; Hosono, H.; Sadakata, M. *Appl. Phys. Lett.* **2002**, *80*, 4259−4261.
(15) Hosono, H.; Abe, Y. *Inorg. Chem.* **1987**, *26*, 1192−*1195*.
(16) Hayashi, K.; Matsuishi, S.; Kamiya, T.; Hirano, M.; Hosono, H. *Nature* **2004**, *419*, 462−465.
(17) Hayashi, K.; Matsuishi, S.; Ueda, N.; Hirano, M.; Hosono, H. *Chem. Mater.* **2003**, *15*, 1851−1854.
(18) Yang, S.; Konda, J. N.; Hayashi, K.; Hirano, M.; Domen, K.; Hosono, H. *Chem. Mater.* **2004**, *16*, 104−110.
(19) Matsuishi, S.; Toda, Y.; Miyakawa, M.; Hayashi, K.; Kamiya, T.; Hirano, M.; Tanaka, I.; Hosono, H. *Science* **2003**, *301*, 626−629.
(20) Hayashi, K.; Hirano, M.; Matsuishi, S.; Hosono, H. *J. Am. Chem. Soc.* **2002**, *124*, 738−739.
(21) Li, Q. X.; Hosono, H.; Hirano, M.; Hayashi, K.; Nishioka, M.; Kashiwagi, H.; Torimoto, Y.; Sadakata, M. *Surf. Sci.* **2003**, *527*, 100−112.
(22) Li, J.; Huang, F.; Wang, L.; Yu, S. Q.; Torimoto, Y.; Sadakata, M.; Li, Q. X. *Chem. Mater.* **2005**, *17*, 2771−2774.
(23) Li, J.; Huang, F.; Wang, L.; Wang, Z. X.; Yu, S. Q.; Torimoto, Y.; Sadakata, M.; Li, Q. X. *J. Phys. Chem. B* **2005**, *109*, 14599−14603.
(24) Deubel, D. V.; Frenking, G. *J. Am. Chem. Soc.* **1999**, *121*, 2021−2031.
(25) Fessenden, R. W.; Meisel, D. *J. Am. Chem. Soc.* **2000**, *122*, 3773−3774.
(26) Lee, J.; Grabowski, J. *J. Chem. Rev.* **1992**, *92*, 1611−1647.
(27) Born, M.; Ingemann, S.; Nibbering, N. M. M. *Mass Spectrom. Rev.* **1997**, *16*, 181−200.
(28) Tashiro, T.; Watanabe, T.; Kawasaki, M.; Toi, K. *J. Chem. Soc., Faraday Trans.* **1993**, *89*, 1263−1269.
(29) Aika, K. I.; Lunsford, J. H. *J. Phys. Chem.* **1977**, *81*, 1393−1398.
(30) Neophytides, S. G.; Tsiplakides, D.; Stonehart, P.; Jaksic, M. M.; Vayenas, C. G. *Nature* **1994**, *370*, 45−47.
(31) Pant, K. K.; Kunzru, D. *Chem. Eng. J.* **2002**, *87*, 219−225.
(32) Lemonidou, A. A.; Vasalos, I. A. *Appl. Catal.* **1989**, *54*, 119−138.
(33) Lemonidou, A. A.; Koulouris, A. P.; Varvarezos, D. K.; Vasalos, I. A. *Appl. Catal.* **1991**, *69*, 105−123.
(34) Dong, T.; Li, J.; Huang, F.; Wang L.; Tu, J.; Torimoto, Y.; Sadakata, M.; Li, Q. X. *Chem. Commun.* **2005**, *21*, 2724−2726.
(35) Basu, B.; Kunzru, D. *Ind. Eng. Chem. Res.* **1992**, *31*, 146−155.
(36) Goula, M. A.; Lemonidou, A. A.; Grünert, W.; Baerns, M. *Catal. Today* **1996**, *32*, 149−156.
(37) Yang, S.; Kondo, J. N.; Hayashi, K.; Hirano, M.; Domen, K.; Hosono, H. *Appl. Catal., A* **2004**, *277*, 239−246.
(38) Kumar, V. A.; Pant, K. K.; Kunzru, D. *Appl. Catal., A* **1997**, *162*, 193−200.
(39) Pant, K. K.; Kunzru, D. *Ind. Eng. Chem. Res.* **1997**, *36*, 2059−2065.
(40) Pant, K. K.; Kunzru, D. *Chem. Eng. J.* **2002**, *87*, 219−225.
(41) Pant, K. K.; Kunzru, D. *Chem. Eng. J.* **1998**, *70*, 47−54.
(42) Gao, A. M.; Zhu, X. F.; Wang, H. J.; Tu, J.; Lin, P. Y.; Torimoto, Y.; Sadakata, M.; Li, Q. X. *J. Phys. Chem. B* **2006**, *110*, 11854−11862.
(43) Olive, H. G.; Olive, S. *The Chemistry of the Catalyzed Hydrogenation of Carbon Monoxide*; Springer-Verlag: Tokyo, 1984; pp 144.

and carbon-neutral alternative to conventional diesel, kerosene, and gasoline.[1,44,45]

In principle, syngas can be produced from many hydrocarbon feedstocks, including natural gas, naphtha, residual oil, petroleum coke, coal, and biomass. Many process configurations for the conversion of biomass to syngas are possible, such as biomass gasification[6,7] and the steam reforming of bio-oil.[46−49] There were several groups that had reported about the production of hydrogen and/or hydrogen-rich syngas via the steam reforming of bio-oil.[46−49] The composition of syngas derived from the steam reforming reaction of bio-oil is much different from that of the conventional syngas used in industry. The latter mainly consists of H_2 and CO with a small amount of CO_2, whereas bio-oil-syngas generally consists of a much greater amount of CO_2, resulting in a higher CO_2/CO ratio and lower $H_2/(CO + CO_2)$ ratio. The composition of bio-oil-syngas also depends on the parameters of steam reforming reactions such as temperature, steam-to-carbon (S/C) ratio, catalyst types, and so forth. Generally, the adjusted bio-oil-syngas with a composition of $H_2/(2CO + 3CO_2) > 1.0$ should be more favorable for FTS processes,[50] which can be tailored in the downstream process by methane reforming (converts CH_4 with steam to CO and H_2), the water−gas shift (WGS) reaction (adjusts the H_2/CO ratio by converting CO with steam to H_2 and CO_2), CO_2 removal, and so forth. To maximize the effective utilization of C sources in the bio-oil-syngas, the steam reforming of bio-syngas with additional natural gas feedstock has been developed recently.[49] However, the capital cost for syngas generation will be very high considering the adjusting steps. Therefore, simplification in syngas production would significantly improve the overall process economics. A new possible way is the direct employment of bio-oil-syngas for the production of FT hydrocarbons via one pass through the reactor using unconverted syngas to coproduce electricity in a gas turbine combined cycle.

In the present work, the characteristics of the bio-oil-syngas and bio-oil reforming performance (the hydrogen yield, carbon conversion, and main composition of the bio-oil-syngas) have been investigated using three different reforming catalysts (C12A7/15%Mg, 12%Ni/γ-Al_2O_3, and 1%Pt/γ-Al_2O_3). Fischer−Tropsch synthesis has been carried out in a fixed-bed flow reactor by using the $H_2/CO/CO_2/N_2$ mixture as a model bio-oil-syngas. The main purpose of the present study is not only to study bio-oil-syngas production and FTS via CO_2-rich bio-oil-syngas but also to develop an economic approach to directly produce clean liquid biofuel from bio-oil.

2. Experimental Section

2.1. Catalyst Preparation. For preparing the MgO-doped C12A7 (C12A7/Mg) catalyst, we first synthesized the C12A7 catalyst, which has been described in detail previously.[14] Briefly, C12A7 was synthesized by the solid-state reactions of $CaCO_3$ and γ-Al_2O_3 under a flowing O_2 atmosphere. The powders of $CaCO_3$ and γ-Al_2O_3 with an average particle diameter of 20−40 μm were mixed and grained at a molar ratio of $CaCO_3/\gamma$-Al_2O_3 = 12:7. The powder mixture was pressed to a pellet with a diameter of 15 mm and a thickness of 1 mm using a pressure of 150−200 kg/cm^2. The pellet samples were temperature-programmed to 1350 °C with a heating rate of 10 °C/min and then calcined at 1350 °C for 16 h under a flowing O_2 atmosphere (flow rate: 50 mL/min). The calcined samples were naturally cooled to room temperature and finally formed the C12A7 samples. For preparing the C12A7/Mg catalyst, the C12A7 sample was powdered (average particle diameter: 20−40 μm) and mechanically mixed with various contents of MgO (average particle diameter: 20−40 μm). Then, the mixture was calcined in the air at 900 °C for 4 h by a muffle furnace. This series of materials was defined as C12A7/*x*%Mg (*x* = the weight percent of magnesium in the samples). Finally, all the calcined C12A7/Mg samples were crushed into granules (180−250 μm) and used for steam reforming reactions. It was found that C12A7/15%Mg showed high activity for bio-oil steam reforming.

A nickel catalyst supported on γ-Al_2O_3 was prepared by the wet impregnation method using nickel nitrate as the metal precursor. A known amount of $Ni(NO_3)_2$ was dissolved in water, and γ-Al_2O_3 was added to the solution under continuous stirring. The slurry was dried at 110 °C for 24 h and then calcined in the air at 500 °C for 2 h for complete decomposition of the nickel nitrate. After this treatment, the catalyst samples were reduced at 500 °C in a H_2 flow for 5 h. The nickel loading was 12 wt % (12%Ni/γ-Al_2O_3).

A platinum catalyst was prepared by impregnation of the support γ-Al_2O_3 with an aqueous solution of the metal precursor H_2PtCl_6. The slurry was dried at 110 °C for 24 h and then reduced at 700 °C in a H_2 flow for 2 h. The platinum loading of the catalyst was 1 wt %.

The Fe/Cu/Al/K catalysts were prepared by using a continuous coprecipitation method. The catalyst precursor was precipitated from an aqueous solution containing iron, copper, and aluminum nitrates at the desired Fe/Cu/Al ratio using aqueous ammonia as a precipitator at a constant pH of 7.0 and a constant temperature of 80 °C. The obtained precipitation was filtered and washed three times with deionized water, then dried at 110 °C for 24 h in a vacuum oven. After a drying step, the potassium promoter was added as aqueous $KHCO_3$ solution via an incipient wetness pore-filling technique. The final step was to dry the catalysts at 110 °C for 24 h in a vacuum oven and then calcine them at 450 °C for 6 h.

Finally, all the calcined catalysts were crushed into granules (180−250 μm), which were then used as catalysts to investigate the steam reforming of bio-oil and Fischer−Tropsch synthesis.

2.2. Catalyst Characterization. The final magnesium content in the Mg-doped C12A7 catalyst and the Ni and Pt content in the prepared catalysts (Ni/γ-Al_2O_3 and Pt/γ-Al_2O_3) were measured by an inductively coupled plasma and atomic emission spectroscopy (ICP/AES) system (Atom Scan Advantage of Thermo Jarrell Ash Corporation, USA).

The element composition of the bulk of the prepared Fe/Cu/Al/K catalyst was also detected by ICP/AES. The surface atomic composition of the prepared Fe/Cu/Al/K catalyst was detected by X-ray photoelectron spectroscopy. The Brunauer−Emmett−Teller (BET) surface area and pore volume were determined by N_2 physisorption at −196 °C using a COULTER SA 3100 analyzer.

To investigate the reducibility performance and the metal−support interaction of the Fe/Cu/Al/K catalyst, temperature-programmed reduction (TPR) experiments were carried out in a quartz microreactor loaded with 50 mg of the catalyst. The catalyst was initially flushed with argon at 50 °C for 30 min. Then, the reducing gas, a mixture of 5% H_2 diluted by argon, was switched on at a flow rate of 50 mL/min via a mass flow controller. The temperature was increased to a rate of 5 °C/min until a temperature of 800 °C was reached. The water produced by the reduction was trapped on a 5 Å molecular sieve. The consumption of H_2 during the reduction was monitored using a thermal conductivity detector [TCD; ultrahigh-purity argon (99.999%) used as carrier gas].

(44) Larson, E. D.; Jin, H. *Proceedings of the Fourth Biomass Conference of the Americas*; Elsevier Science: Kidlington, U.K., 1999; Vol. 1/2, pp 843−854.

(45) Hamelinck, C. N.; Faaij, A. P. C.; Uil, H. d.; Boerrigter, H. *Energy* **2004**, *29*, 1743−1771.

(46) Kechagiopoulos, P. N.; Voutetakis, S. S.; Lemonidou, A. A.; Vasalos, I. A. *Energy Fuels* **2006**, *20*, 2155−2163.

(47) Garcia, L.; French, R.; Czernik, S.; Chornet E. *Appl. Catal., A* **2000**, *201*, 225−239.

(48) Rioche, C.; Kulkarni S.; Meunier, F. C.; Breen, J. P.; Burch, R. *Appl. Catal., B* **2005**, *61*, 130−139.

(49) Czernik, S.; French, R.; Feik, C.; Chornet, E. *Ind. Eng. Chem. Res.* **2002**, *41*, 4209−4215.

(50) Dry, M. E. *Appl. Catal., A* **1996**, *138*, 319−344.

Table 1. The Elemental Compositions and Characteristics of Bio-Oils Derived from the Sawdust, Rice Husk, and Cotton Stalk Powder

bio-oil from different feedstocks	element (wt %) C	H	O	H_2O (wt %)	ash (wt %)	density (kg/m^3)	LHV (MJ/kg)	pH
sawdust	54.5	6.7	38.7	21.0	0.07	1300	18.20	2.1
rice husk	41.0	7.4	51.2	24.5	0.08	1150	17.16	3.2
cotton stalk	42.3	7.9	49.4	24.4	0.07	1160	17.77	3.3

Table 2. Some Chemical Properties of Crude Bio-Oil and the Pretreated Bio-Oil

composition (wt %)	crude bio-oil	pretreated bio-oil
H_2O	21.0	34.5
elemental composition, wt %		
C	54.5	51.6
H	6.7	7.8
O	38.7	40.5
chemical formula	$CH_{1.48}O_{0.53}\cdot 0.32H_2O$	$CH_{1.82}O_{0.59}\cdot 0.68H_2O$

X-ray diffraction (XRD) measurements were employed to investigate the bulk structure of the prepared Fe/Cu/Al/K catalyst. The catalysts are generally crushed into powder with an average diameter of 20−30 μm. Powder X-ray diffraction patterns were recorded on an X'pert Pro Philips diffractometer with a Cu Kα source. The measurement conditions were in the 2θ range of 10−80°, using a step counting time of 5 s and step size of 0.017° at room temperature.

2.3. Bio-Oil. Bio-oil, also called pyrolysis oil or pyrolysis liquid, was produced by the fast pyrolysis of biomass in a circulating fluidized bed with a capacity of 120 kg/h of oil at the Anhui Province Key Laboratory of the Biomass Clean Energy (patent: ZL01263584.7). The pyrolysis temperature ranged from 420 to 540 °C, which was supplied by the byproducts of charcoal formed in the bio-oil production process. The pyrolysis of biomass was generally performed with a heating rate of about 10^4 °C/s for a residence time of less than 2 s and was followed by a fast cooling process. The main products of the fast pyrolysis of biomass consisted of liquid bio-oil (55∼70 wt %), a mixture gaseous products (e.g., CO_2, CO, CH_4, etc.), and charcoal.

Bio-oils are dark-brown organic liquids and comprise different molecular weight products derived from depolymerization and fragmentation reactions of three key biomass building blocks: cellulose, hemicellulose, and lignin. Therefore, the elemental composition of bio-oil varied with different feedstocks of biomass. Some physical and chemical properties of the bio-oils derived from the sawdust, rice husk, and cotton stalk powder were summarized in Table 1. The bio-oils contain a large number of complex compounds such as hydroxyaldehydes, hydroxyketones, sugars, carboxylic acids, phenolics, and so forth. The distribution of these compounds depends on the type of biomass used and on the pyrolysis process conditions (temperature, residence time, and heating rate). Because the main elemental composition of the pyrolysis bio-oils was C, H, and O (see Table 1), we described the oxygenated organic compounds in the pyrolysis bio-oils with a chemical formula of $C_nH_mO_k\cdot xH_2O$. As for bio-oil derived from sawdust, the chemical formula is $CH_{1.48}O_{0.53}\cdot 0.32H_2O$ (see Table 2). In this work, the volatile organic components of the crude bio-oil derived from sawdust (see section 2.4) were used for steam reforming experiments.

2.4. Reaction System and Operating Procedure. The bio-oil derived from sawdust is a complex mixture including carboxylic acids, aldehydes, alcohols, lignin-derived aromatic phenolics, and so forth. The crude pyrolysis oil contains substantial amounts of nonvolatile materials (35−40 wt %), such as sugars, oligomeric phenolics, and so forth, which are generally difficult to reform. Particularly, these nonvolatile materials easily form carbon depositions on the catalyst surface and lead to the fast deactivation of catalysts when the crude oil is directly fed into the reforming reactor. Thus, in this work, the volatile organic components of the crude bio-oil, prepared by vaporing the crude bio-oil from 80 °C to 200 °C, were used for the steam reforming experiments. The amount of pretreated bio-oil (the volatile organic components of the crude bio-oil) was about 50−60 wt % of the crude oil. As shown in Table 2, the oxygenated organic compound in the pretreated bio-oil was represented using a chemical formula of $CH_{1.82}O_{0.59}\cdot 0.68H_2O$.

As shown in Figure 1a, the bio-oil steam reforming experiments were carried out in a continuous flow system using a fixed-bed microreactor under atmospheric pressure. The catalyst powder (200 mg) was adjusted to the middle zone of the furnace to get a homogeneous temperature. The reaction system was equipped with pressure indicators and mass flow controllers. The pretreated bio-oil (i.e., the volatile organic components of the crude bio-oil) was enclosed in a vessel (200 mL) and was kept at 150 °C. The vapor of the pretreated bio-oil was fed into the reactor using N_2 (99.999%) as the carrier gas. To obtain a relatively stable carbon feeding, a flowing feed-eduction system was designed where the pretreated bio-oil was supplied online from a large oil tank (10 L), and the flow rate was controlled by the valves. Before performing the reforming experiments, we first collected the feeding oil vapor with an ice-cooled conical flask every 10 min. The data of weight, volume, and elemental composition for each collection were measured. The main elemental compositions of C, H, and O in all collected oils were almost constant with an error of ±10%. This means that the carbon feeding using the flowing feed-eduction system was almost stable, which also agree with the results of time on stream for the reforming experiments as well as the estimation of the material balance as described below. On the other hand, steam was simultaneously fed into the reactor for adjusting the S/C ratio (molar ratio of steam to carbon fed), and the steam amount was also calibrated before running the reforming experiments.

FTS was investigated in a 1 cm i.d. stainless steel fixed-bed flow reactor (Figure 1b). The catalyst (1.5 g) was loaded into the reactor and diluted with inert silica sand of the same particle size. The volume ratio of catalyst to silica sand was 1:8. Thus, a uniform gas flow at a low-pressure drop could be achieved, and the high degree of catalyst dilution with the inert material allowed for operation at almost isothermal conditions.[51] The catalyst precursor was reduced in situ in a flow of ultrahigh-purity hydrogen at 400 °C for 12 h under 3 atm. The flow rate of hydrogen was maintained at 90 mL/min. After the temperature cooled down to the reaction temperature, the bio-oil-syngas was fed into the reactor. The reaction temperature was measured by a thermocouple inserted into the catalyst bed. The feeding gas and reducing gas were individually measured and controlled by mass flow controllers. High-molecular-weight hydrocarbon products (wax) were collected in a hot condenser (keept at about 150 °C) located directly downstream of the reactor (see Figure 1b). The product tubes between the reactor outlet and hot condenser were heated at 200 °C to prevent product condensation. Then, the remaining condensable products passed through a water-cool vessel and were collected in a cold condenser (keept at about 0 °C). The C_{5+} hydrocarbons collected both in the hot condenser and in the cold condenser were analyzed periodically by a gas chromatograph (mode: SP-6800A) installed with a capillary column (SE-30, uniport) and a flame ionization detector (FID). Finally, the tail gas (the reactants and noncondensable products) from the cold condenser was analyzed by online gas chromatographs with flame ionization and thermal conductivity detectors (see section 2.5). Moreover, the flow rate of the tail gas was measured periodically by using a soap film flowmeter.

(51) Riedel, T.; Schaub, G.; Jun, K. W.; Lee, K. W. *Ind. Eng. Chem. Res.* **2001**, *40*, 1355−1363.

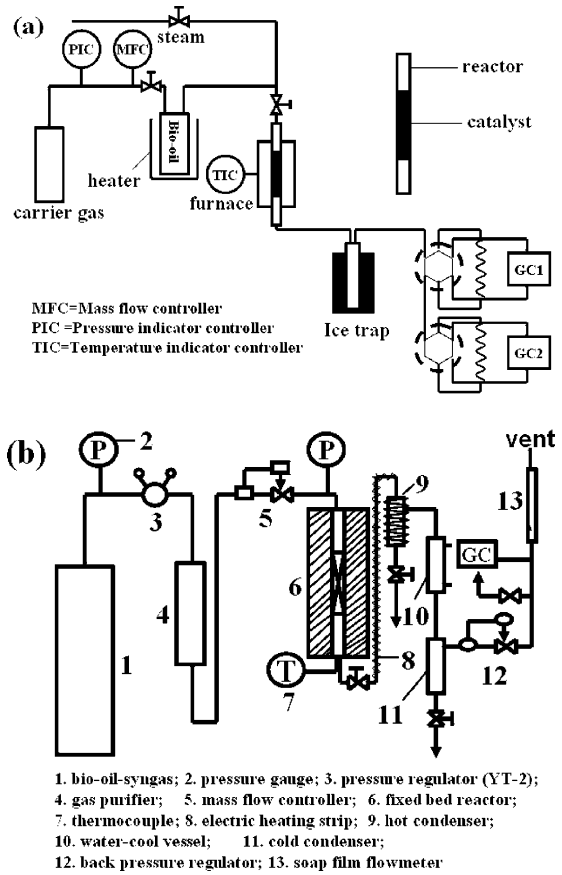

Figure 1. (a) Schematic setup of the fixed-bed flow microreactor system for the steam reforming of the pretreated bio-oil. (b) Schematic diagram of the experimental apparatus for Fischer−Tropsch synthesis using the bio-oil-syngas.

2.5. Analysis of the Products. The products of bio-oil steam reforming were analyzed by two online gas chromatographs (GC1 and GC2, as shown in Figure 1a) with TCD, using ultrahigh-purity argon (99.999%) as a carrier gas. H_2, CO, and CH_4 were detected by GC1 (molecular sieve 5 Å). CO_2 was detected by GC2 (GDX-502). The composition of the reactor gaseous effluent was also confirmed by a Q-MS mass spectrometer (mode: GSD 300 Omnistar).

The bio-oil reforming performance on a given catalyst was studied by measuring hydrogen yield, carbon conversion, and dry gas composition under variable reforming conditions (i.e., temperature, S/C ratio, types of reforming catalyst, etc.). The hydrogen yield was calculated as a percentage of the stoichiometric potential, in case of complete conversion of the elemental carbon in the bio-oil to CO_2 according to reaction 3. Thus, the potential yield of hydrogen is $2 + m/2n - k/n$ moles per mole of carbon in the feed. The carbon conversion was calculated by the total moles of carbon in the gaseous products divided by the moles of carbon in the fed bio-oil (i.e., the ratio of the moles of carbon in gas to the carbon fed). Generally, all experiments were repeated three times. The difference for each repeating, in general, ranged from 0 to 10%.

Gaseous reactants and products of FTS were analyzed with two online gas chromatographs (SP-6800A). H_2, N_2, CO, CO_2, and CH_4 were analyzed on the TCD after separation by a carbon molecular sieve column (TDX-01), using ultrahigh-purity argon (99.999%) as a carrier gas. Light hydrocarbons (C_1−C_4) were separated with a Porapack-Q column and detected on the FID. The composition of the reactor effluent was also confirmed by the Q-MS mass spectrometer (mode: GSD 300 Omnistar). C_{5+} hydrocarbons were analyzed using a capillary column (SE-30, uniport). The carbon oxide reactants conversion denoted as X_{reactant}, and products selectivity (CH_4, C_2−C_4 and C_{5+}) denoted as S_{product}, are calculated by the following formulas:

$$X_{\text{reactant}}(\%) = \frac{\text{moles of reactant}_{\text{in}} - \text{moles of reactant}_{\text{out}}}{\text{moles of reactant}_{\text{in}}} \times 100\% = \frac{(\text{reactant/N}_2)_{\text{in}} - (\text{reactant/N}_2)_{\text{out}}}{(\text{reactant/N}_2)_{\text{in}}} \times 100\%$$

"reactant" stands for CO, CO_2, and total carbon ($CO + CO_2$).

$$S_{CH_4}(\%) = \frac{\text{moles of CH}_{4_{\text{produced}}}}{\text{moles of (CO + CO}_2)_{\text{in}} - \text{moles of (CO + CO}_2)_{\text{out}}} \times 100\%$$

$$S_{C_n}(\%) = \frac{n \times \text{moles of C}_{n_{\text{produced}}}}{\text{moles of (CO + CO}_2)_{\text{in}} - \text{moles of (CO + CO}_2)_{\text{out}}} \times 100\%$$

C_n stands for a hydrocarbon that contains n carbon, $n = 2$, 3, and 4.

$$\text{olefin in } (C_2 - C_4) = \frac{\text{moles of olefin in } (C_2 - C_4)}{\text{moles of } (C_2 - C_4) \text{ hydrocarbon}} \times 100\%$$

$$S_{C_{5+}}(\%) = 100\% - \sum(S_{CH_4} + S_{C2} + S_{C3} + S_{C4})$$

It should be pointed out that all the data of FTS were almost constant for 100 h of experiments under the investigated reaction conditions. For investigating the effect of reaction conditions [temperature, total pressure, W/F (W and F stand for weight of catalyst and molar feed rate of the model syngas, respectively) and $CO_2/(CO+CO_2)$ ratio] on catalytic activity and hydrocarbon product selectivity, all of the data presented were given as the average value, derived from the stable region.

3. Results and Discussion

3.1. Production of Bio-Oil-Syngas. To investigate the features of the bio-oil-syngas, we performed the catalytic steam reforming of the bio-oil over three different catalysts, that is, Mg-doped C12A7 catalyst, Ni-based catalyst, and Pt-based catalyst. Steam reforming of the bio-oil can be simplified as the catalytic steam reforming of the oxygenated organic compound ($C_nH_mO_k$) by the following reaction:

$$C_nH_mO_k + (n - k)\,H_2O = nCO + (n + m/2 - k)H_2 \quad (1)$$

The above reaction is followed by the WGS reaction:

$$nCO + nH_2O = nCO_2 + nH_2 \quad (2)$$

Therefore, the overall process can be represented as follows:

$$C_nH_mO_k + (2n - k)H_2O = nCO_2 + (2n + m/2 - k)H_2 \quad (3)$$

The most important parameters for the steam reforming of bio-oil are the reforming temperature (T), the molar ratio of steam to carbon fed (S/C), and the reforming catalysts. Table 3 shows the effects of the reforming temperature on the hydrogen yield, the carbon conversion (moles of carbon in gas-phase products to moles of carbon fed), and dry gas composition (i.e., H_2, CO, CO_2, CH_4) over three different reforming catalysts (i.e., C12A7/15%Mg, 12%Ni/γ-Al_2O_3, and 1%Pt/γ-Al_2O_3). When the temperature was lower than 450 °C, the H_2 yields were low (<5%) for all tested catalysts. With temperature increasing, both the H_2 yield and the carbon conversion increased in our investigated range over all three of the reforming catalysts. The 1%Pt/γ-Al_2O_3 catalyst performed better (i.e., highest H_2 yield and highest carbon conversion) than the other tested catalysts under

Table 3. The Effect of Reaction Temperature on the Performance of the Bio-Oil Steam Reforming Reaction and Dry Gas Composition of the Bio-Oil-Syngas over Three Various Catalysts[a]

				dry gas composition (%)			
catalyst	*T* (°C)	carbon conversion (%)	H_2 yield (st. %)	H_2	CO	CO_2	CH_4
C12A7/15%Mg	500	15.6	47.1	52.2	1.8	35.9	10.1
	600	42.7	53.3	55.3	2.7	34.3	7.7
	650	59.2	56.7	56.8	3.8	32.3	7.1
	700	80.3	63.6	59.6	5.6	29.6	5.2
	750	93.4	70.6	62.1	8.0	25.2	4.7
12%Ni /γ-Al_2O_3	650	40.4	58.1	57.4	2.6	32.6	7.4
	750	81.2	66.0	60.5	4.8	29.7	5.0
	850	97.0	71.5	62.4	9.0	25.3	3.3
1%Pt/γ-Al_2O_3	600	52.6	60.0	58.2	2.1	34.2	5.5
	650	76.5	66.8	60.8	6.0	28.7	4.5
	700	98.3	75.0	63.5	12.0	22.8	1.7

[a] Reforming conditions: 200 mg of catalyst, $S/C = 6.0$, and GHSV = 26 000 h^{-1}.

Table 4. The Effect of *S/C* on the Performance of the Bio-Oil Steam Reforming Reaction and Dry Gas Composition of the Bio-Oil-Syngas over C12A7/15%Mg Catalyst[a]

			dry gas composition (%)					
S/C	carbon conversion (%)	H_2 yield (st. %)	H_2	CO	CO_2	CH_4	$H_2/(CO+CO_2)$	CO_2/CO
1.5	81.2	55.5	56.3	13.4	22.3	8.0	1.58	1.66
6.0	93.4	70.6	62.1	8.0	25.2	4.7	1.87	3.15
15.0	97.8	77.6	64.3	2.9	29.3	3.5	2.0	10.1

[a] Reforming conditions: 200 mg of catalyst, $T = 750$ °C, and GHSV = 26 000 h^{-1}.

the same reforming conditions. However, such noble-metal-based catalysts are not common in real applications because of their high cost. The C12A7/15%Mg catalyst also gave a higher yield of hydrogen under the optimum steam reforming conditions. For the C12A7/15%Mg catalyst, a hydrogen yield of about 71% was obtained, and the maximum carbon conversion was about 93% at $T = 750$ °C and S/C = 6.0. Conventional steam reforming catalysts for hydrocarbons (e.g., methane) are 10−33 wt % NiO on a mineral support, which operate at 800−850 °C, and the reforming S/C ratio is usually 4−6.[52] The maximal conversion efficiency of the pretreated bio-oil (the carbon conversion and the yield of hydrogen) by using the C12A7/15%Mg catalyst was close to that using the Ni-based catalysts, but the C12A7/15%Mg catalyst possesses some advantages such as a lower steam reforming temperature.

It was observed that the reforming temperature and the S/C ratio had the most profound effect on the catalytic steam reforming process of the bio-oil. For the C12A7/15%Mg catalyst, the hydrogen yield is lower than 5% at temperatures below 450 °C. In the temperature range of 500∼750 °C, the hydrogen yield significantly increases with increasing temperature, giving a maximum value of about 71% within our investigated region. The carbon conversion was about 15% at 500 °C and reached about 93% at 750 °C with S/C = 6.0 and a gas hourly space velocity (GHSV) of 26 000 h^{-1}. On the other hand, both the hydrogen yield and the carbon conversion obviously increased as the S/C ratio increased from 1.5 to 6.0 and increased slightly from 6.0 to 15.0 (Table 4). As mentioned above, the chemical processes of bio-oil steam reforming, commonly occurring in the reformer, include the steam reforming reaction of oxygenated organic compounds with water (reaction 1) and the water−gas shift reaction (reaction 2). The reforming reaction is generally endothermic and is favored by high temperatures, leading to a higher carbon conversion and H_2 yield at higher temperatures. In contrast, the water−gas shift reaction is exothermic and favors low temperatures.

Moreover, the stability of the reforming reactions was investigated by measuring the yield of hydrogen and the carbon conversion as a function of time on stream using the C12A7/15%Mg catalyst. Figure 2a and b show the typical curves measured at 750 °C, S/C = 6.0, and GHSV = 26 000 h^{-1}. As can be seen, the hydrogen yield and the carbon conversion remained almost constant in the initial time on stream of 120 min. Then, a gradual decrease of the yield of hydrogen as well as the carbon conversion was observed. When a fresh sample was used as a catalyst for the steam reforming reaction under the same reaction conditions, it was found that the hydrogen yield and the carbon conversion returned to almost the same degree. It indicates that the decrease of the hydrogen yield as well as the carbon conversion are attributed to the deactivation of the catalyst by carbon deposition.

The material balance was estimated for the initial reforming duration of 2 h. Table 5 presents the overall material balance of the pretreated bio-oil steam reforming reactions. The overall material balance, defined as the ratio of outlet mass to inlet mass (in wt %), was 100 ± 8% for all experiments. Thus, the overall material balance of the pretreated bio-oil steam reforming reactions nearly closes under the present experimental conditions.

The present results show that H_2 and CO_2 are the major products of bio-oil steam reforming together with small amounts of CO and CH_4 in the effluent gaseous compounds. As shown in Tables 3 and 4, the dry gas composition also depends on the reforming temperature, the S/C ratio, and the catalyst type. In order to more clearly show the composition distribution of the bio-oil-syngas, the volume ratios of $H_2/(CO + CO_2)$ and CO_2/CO were depicted as a function of the reaction temperature for the catalytic steam reforming of the bio-oil over three different reforming catalysts (i.e., C12A7/15%Mg, 12%Ni/γ-Al_2O_3, and 1%Pt/γ-Al_2O_3; Figure 3). As can be seen from Figure 3a, the volume ratio of $H_2/(CO + CO_2)$ ranges from 1.49 to 1.87 and

(52) Satterfield, C. N. *Heterogeneous Catalysis in Industrial Practice*; McGraw-Hill: New York, 1991; pp 427.

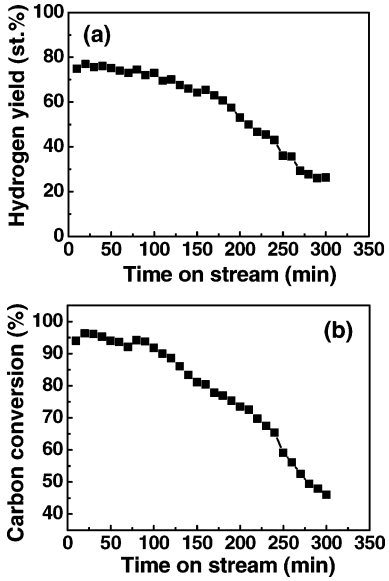

Figure 2. Effect of time on stream on (a) the hydrogen yield (st. %) and (b) the carbon conversion for steam reforming of the pretreated bio-oil over a C12A7/15%Mg catalyst. Steam reforming conditions: 200 mg of catalyst, $S/C = 6.0$, and GHSV $= 26\,000\ h^{-1}$.

Table 5. Overall Material Balance Estimated from the Steam Reforming of the Pretreated Bio-Oil over C12A7/15%Mg, 12%Ni/γ-Al_2O_3, and 1%Pt/γ-Al_2O_3[a]

	outlet mass/inlet mass (wt %)		
product distribution	C12A7/15%Mg[b]	12%Ni /γ-Al_2O_3[c]	1%Pt/γ-Al_2O_3[d]
CO	4.0	4.8	6.5
CO_2	19.8	20.8	19.6
H_2	2.2	2.4	2.5
CH_4	1.3	1.0	0.6
coke	0.9	1.4	0.7
residue	1.1	0.5	0.3
H_2O	65.8	72.1	62.2
total	95.1	103.0	92.4

[a] Reforming conditions: $S/C = 6.0$ and GHSV $= 26\,000\ h^{-1}$, 200 mg of catalyst, time on stream = 120 min. [b] $T = 750$ °C [c] $T = 850$ °C [d] $T = 700$ °C.

gradually increases with increasing temperature in our investigated region of 600∼850 °C over all three of the catalysts. Particularly, the CO_2/CO ratio is higher than 1.0 (Figure 3b), which indicates that the bio-oil-syngas derived from the catalytic steam reforming of the bio-oil is a CO_2-rich syngas. For the C12A7/15%Mg catalyst, the CO_2/CO ratio sharply decreases from about 12.7 to 7.7 as the temperature rises from 600 to 650 °C and further decreases to 3.2 at higher steam reforming temperatures ($T = 750$ °C). As shown in Table 4, with an increase of the S/C ratio from 1.5 to 15, the ratio of $H_2/(CO + CO_2)$ increases from about 1.6 to 2.0, and the CO_2/CO ratio increases from about 1.7 to 10.1 simultaneously. The above results indicated that a higher S/C ratio was necessary to ensure a high carbon-to-gas conversion and favorably shift the water−gas shift equilibrium. On the other hand, a small amount of methane was detected in the products of bio-oil steam reforming. Methane was most likely formed by the thermal cracking of oxygenated organic compounds, which always accompanies the catalytic reforming reaction. Methane in the bio-oil-syngas can be considered to be an inert gas in the FTS process. The existence of methane in the syngas will decrease the effective partial pressure of H_2, CO, and CO_2. To simplify the synthesis process, according to the above investigation, mixtures of H_2/CO/CO_2 balanced by N_2 were employed as the model bio-oil-syngas in the following FTS processes.

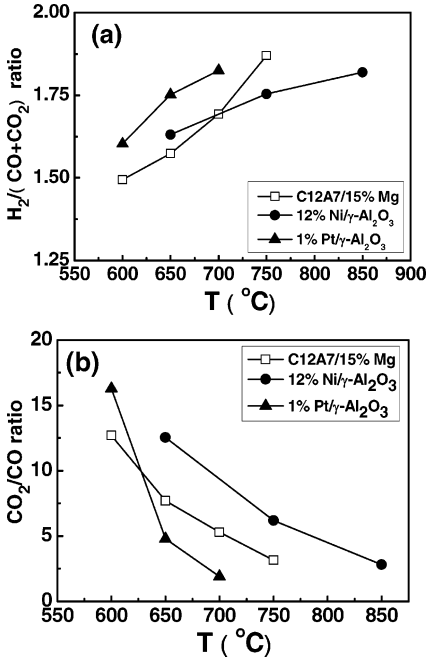

Figure 3. (a) Ratio of $H_2/(CO + CO_2)$ and (b) the ratio of CO_2/CO measured as a function of temperature for steam reforming of the pretreated bio-oil over three catalysts (C12A7/15%Mg, 12%Ni/γ-Al_2O_3, 1%Pt/γ-Al_2O_3). Steam reforming conditions: 200 mg of catalyst, $S/C = 6.0$, and GHSV $= 26\,000\ h^{-1}$.

3.2. Conversion of Bio-Oil-Syngas to Liquid Biofuel. *3.2.1 Screen and Characterization of Fe/Cu/Al/K FTS Catalysts.* For FTS using the bio-oil-syngas, it is very important to select an optimum catalyst. In the present work, we used alumina-supported coprecipitated Fe/Cu/Al/K catalysts for the FTS of the bio-oil-syngas. Generally, group VIII transition metal elements are regarded as good CO hydrogenation catalysts, in decreasing order of activity: Ru > Fe > Ni > Co > Rh > Pd > Pt. Nickel metal is a very active hydrogenation catalyst, and thus, under FT conditions, too much methane is formed, making Ni unsuitable. The earliest catalysts used for FTS were Fe and Co. Ru has very high activity and quite high selectivity for producing high-molecular-weight products at low temperatures, but Ru is about 10^5 times more expensive than Fe. Fe is also very active for FT synthesis with high WGS activity and is by far the cheapest FTS catalyst of all of these metals. Co tends to have a longer lifetime than Fe catalysts but does not have WGS activity. In commercial FTS fixed bed reactors, coprecipitated Fe/Cu/Si/K catalysts have usually been employed.[53,54] However, the catalysts should be readjusted to CO_2-rich feed syngas so that the bio-oil-syngas can be directly used as a feed for hydrocarbon synthesis.

Potassium has been used as a promoter for Fe catalysts to effectively increase the basicity of the catalyst surface. Adding potassium to Fe catalysts also tends to decrease hydrogenation of the adsorbed carbon species, so chain growth is enhanced, resulting in a higher-molecular-weight product distribution that is more olefinic. Potassium is an essential promoter of the catalysts for the WGS reaction and the reverse water−gas shift reaction (RWGS) in FTS reactions. More recently, the K promotion in Fe-based Fischer−Tropsch catalysts was found

(53) Dry, M. E. *Catal. Today* **1990**, *6*, 183−206.
(54) Bukur, D. B.; Lang, X.; Kesh, D.; Zimmerman, W. H.; Rosynek, M. P.; Li, C. *Ind. Eng. Chem. Res.* **1990**, *29*, 1588−1599.

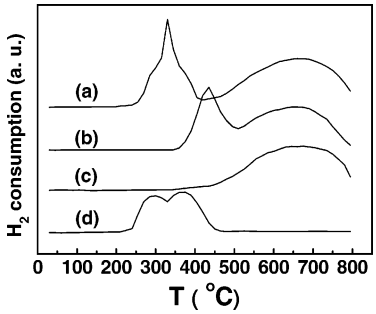

Figure 4. TPR profiles of (a) Fe/Cu/Al/K catalyst, (b) Fe_2O_3, (c) Fe_3O_4, and (d) CuO.

Table 6. Bulk/Surface Composition and Physical Properties of the Coprecipitated Fe/Cu/Al/K Catalyst[a]

catalyst	Fe/Cu/Al/K
bulk composition (wt. ratio)	100Fe/6Cu/16Al/6K
surface composition (wt. ratio)	100Fe/16.7Cu/21.1Al/8.7K
BET surface area (m^2/g)	94.7
pore volume (cc/g)	0.14
mean pore diameter (Å)	59.1

[a] Pore diameter = (4 × pore volume)/surface area.

to be very essential for good catalytic performance in the hydrogenation of CO_2 to hydrocarbon, and relatively high amounts of K were necessary to enhance the CO_2 conversion in Fischer−Tropsch synthesis.[55−57] On the other hand, copper has also been used as a promoter in Fe-based FT catalysts. It increases the rate of FTS more effectively than potassium but decreases the rate of the WGS reaction. Copper has been shown to facilitate iron reduction. The average molecular weight of the products increases in the presence of copper, but not as much as when potassium is used. On the other hand, to obtain higher catalyst dispersion, Al_2O_3 can be used as a structural promoter of iron-based catalysts.[58] As mentioned above, we used alumina-supported coprecipitated Fe/Cu/Al/K catalysts for FTS via the bio-oil-syngas. It was found that the optimum content ratio of Fe/Cu/Al/K was about 100:6:16:6 in weight ratio. The compositions of the bulk/surface and main physical properties of the coprecipitated Fe/Cu/Al/K catalyst used are shown in Table 6.

The reducibility performance and the metal−support interaction of the Fe/Cu/Al/K catalyst were investigated by TPR. The reduction of iron catalysts by hydrogen generally appears through two- or three-staged process.[59] In order to assign the observed TPR peaks of Fe/Cu/Al/K, the reduction features of Fe_2O_3, Fe_3O_4, and CuO were also measured under the same conditions. As shown in Figure 4, there were two distinguishable profiles in the TPR of the Fe/Cu/Al/K catalyst. The first TPR profile ranges from 260 to 400 °C. As compared with the TPR profiles of Fe_2O_3 and CuO, these peaks can be attributed to the simultaneous reduction of CuO to Cu_2O followed by the reduction of Fe_2O_3 to Fe_3O_4 and Cu_2O to Cu. The CuO reduction peaks seem to overlap with that of Fe_2O_3 reduction in the first profile of the Fe/Cu/Al/K catalyst, which implies that the CuO is well-mixed with the Fe_2O_3 phase.[60] Another profile appeared at higher temperatures over 500 °C, which is assigned to the reduction of Fe_3O_4 to α-Fe. The large peak width for the Fe_3O_4 to α-Fe transformation indicates that this is a slow process. It was also found that Cu in the Fe/Cu/Al/K catalyst promotes the reduction of Fe_2O_3 at lower temperatures, which agreed with the previous observation.[61] The promotional effect of Cu was attributed to its ability to dissociate H_2 and provide a source of atomic H to assist in the reduction of Fe_2O_3.

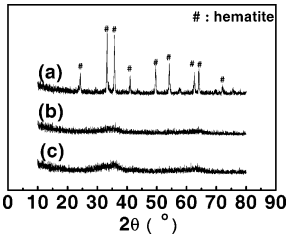

Figure 5. XRD patterns for the coprecipitated catalysts (a) 100Fe/6Cu/6K, (b) 100Fe/6Cu/16Al, and (c) 100Fe/6Cu/16Al/6K.

Moreover, three different samples 100Fe/6Cu/6K, 100Fe/6Cu/16Al, and 100Fe/6Cu/16Al/6K were measured by XRD to investigate the bulk-phase structure characteristics of the catalysts and the dispersion influence via adding alumina and/or potassium. As shown in Figure 5 a, the XRD spectrum for the 100Fe/6Cu/6K sample without the support of alumina appears with several diffraction peaks. By comparing the peak positions and intensities of the XRD pattern with the data in the Joint Committee of Powder Diffraction Standards cards, the main peaks were assigned to the diffraction structure of hematite (Fe_2O_3). As alumina was added to the 100Fe/6Cu/16Al catalyst, however, the diffraction peaks of iron oxide disappeared in the XRD spectrum (Figure 5b). The iron oxide species in the bulk phase of the sample may appear either as small particles (considering the XRD detection limit: <3 nm) or as amorphous particles. Similarly, as potassium was added to the 100Fe/6Cu/16Al/6K catalyst, we have not observed the obvious diffraction peaks of the iron oxide and K_2CO_3 (Figure 5c). Thus, potassium is well-dispersed on the surface of 100Fe/6Cu/16Al/6K via the incipient wetness pore-filling technique, and the addition of alumina to the Fe/Cu/Al/K catalyst promotes the dispersion of the Fe and Cu compositions.

3.2.2. Effect of Temperature on the FTS Reaction. The key factors that influence the FTS process over iron-based catalysts are reaction temperature, pressure, contact time (*W*/*F*), composition of the syngas used, and so forth. Figure 6 presents the FTS results using bio-oil-syngas over the Fe/Cu/Al/K catalyst measured as a function of the temperature at a pressure of 1.5 MPa and a *W*/*F* of 12.5 g_{cat}·h·mol^{-1}. The performance of FTS was evaluated in terms of CO conversion, CO_2 conversion, total carbon (CO + CO_2) conversion, and selectivity of the hydrocarbon products. As shown in Figure 6a, the CO conversion increases with an increase of the reaction temperature at the lower temperature region and reaches a maximum (72.5%) at 300 °C. However, the CO conversion gradually decreases to 61% as the temperature further increases to 340 °C. The CO conversion via the FTS reaction can be recognized as a polymerization reaction with the basic steps of (1) reactant (CO) adsorption on the catalyst surface, (2) chain initiation by CO dissociation followed by hydrogenation, (3) chain growth by the insertion of additional CO molecules followed by hydrogenation, (4) chain termination, and (5) product desorption from

(55) Choi, P. H.; Jun, K. W.; Lee, S. J.; Choi, M. J.; Lee, K.W. *Catal. Lett.* **1996**, *40*, 115−118.
(56) Yan, S. R.; Jun, K. W.; Hong, J. S.; Choi, M. J.; Lee, K. W. *Appl. Catal., A* **2000**, *194*−*195*, 63−70.
(57) Jun, K. W.; Lee, S. J.; Kim, H.; Choi M.; Lee, K. W. *Stud. Surf. Sci. Catal.* **1998**, *114*, 345−350.
(58) Dry, M. E. *The Fischer*−*Tropsch Synthesis*; Springer-Verlag: Berlin, 1981; Vol. 1, pp 159.
(59) Basińska, A.; Jóźwiak, W. K.; Góralski, J.; Domka, F. *Appl. Catal. A* **2000**, *190*, 107−115.
(60) Jin, Y.; Datye, A. K. *J. Catal.* **2000**, *196*, 8−17.
(61) Jun, K. W.; Roh, H. S.; Kim, K. S.; Ryu, J. S.; Lee, K. W. *Appl. Catal., A* **2004**, *259*, 221−226.

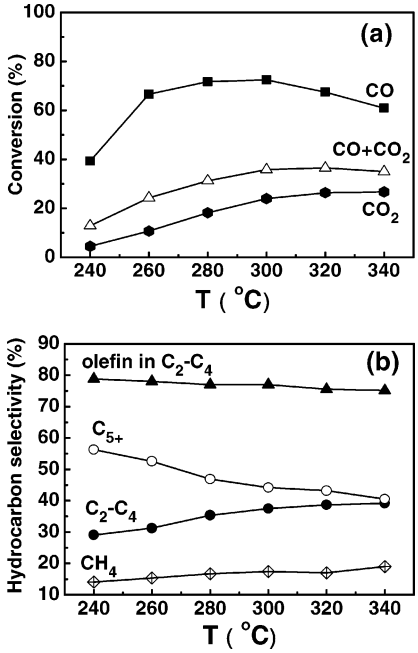

Figure 6. (a) Effect of temperature on CO conversion, CO_2 conversion, and total carbon ($CO + CO_2$) conversion. (b) Effect of temperature on the selectivity of hydrocarbon products. Model bio-oil-syngas: $H_2/CO/CO_2/N_2$ (vol %) = 62:8:25:5. Reaction conditions: $P = 1.5$ MPa, $W/F = 12.5$ g_{cat}·h·mol^{-1}.

the catalyst surface.[62] Chemisorbed methyl species are formed by the dissociation of absorbed CO molecules and the stepwise addition of hydrogen atoms. These methyl species can further hydrogenate to form methane or act as initiators for chain growth to form hydrocarbons. Overall, the FTS reaction via CO hydrogenation over Fe-based catalysts would be represented by the reaction $2CO + H_2 \rightarrow -CH_2- + CO_2$. Thus, the temperature dependence of the CO conversion observed from bio-oil-syngas should partly reflect the features of the above reactions occurring in the FTS process.

The considerable amount of CO_2 contained in the bio-oil-syngas should be pointed out. As shown in Figure 6a, it was also observed that the conversion of CO_2 and the conversion of total carbon ($CO + CO_2$) over the Fe/Cu/Al/K catalyst significantly increased with increasing temperature at the temperature region of $T < 300$ °C. Beyond 300 °C, the CO_2 conversion and ($CO + CO_2$) conversion smoothly increased. For the CO_2 hydrogenation to hydrocarbon over the iron-based catalyst Fe/Cu/Al/K, it would be considered a two-step mechanism: the first step is the conversion of CO_2 to CO via the RWGS reaction (reaction 4), and the subsequent step is the hydrogenation of CO to produce hydrocarbons (reactions 5−7) with CO as an intermediate.[63] Specific FTS processes using the CO_2-rich bio-oil-syngas may be synthesized according to the following reactions:

$$CO_2 + H_2 \rightarrow CO + H_2O \text{ (reverse water−gas shift)} \quad (4)$$

$$nCO + 3nH_2 \rightarrow nCH_4 + nH_2O \text{ (methanation)} \quad (5)$$

$$nCO + (2n + 1)H_2 \rightarrow C_nH_{2n+2} + nH_2O \text{ (paraffins)} \quad (6)$$

$$nCO + 2nH_2 \rightarrow C_nH_{2n} + nH_2O \text{ (olefins)} \quad (7)$$

$$CO + H_2O \rightarrow H_2 + CO_2 \text{ (water−gas shift)} \quad (8)$$

Therefore, the conversion of CO depends not only on the hydrogenation rate of CO (FTS rate) but also on the conversion rate of CO_2 (RWGS rate). In the case of the FTS processes using the CO_2-rich bio-oil-syngas, the CO partial pressure is low, limited by the WGS/RWGS equilibrium. For the RWGS reaction, increasing the temperature would favor the reaction toward the endothermic direction (i.e., CO formation direction). A relatively higher reaction temperature would be favorable for obtaining a higher CO partial pressure, leading to promotion of the Fischer−Tropsch synthesis. CO_2 conversion and total carbon ($CO + CO_2$) conversion, accordingly, increase kinetically as well as thermodynamically with increasing temperature. For the Fischer−Tropsch synthesis reaction, however, it is an exothermic reaction, and the reaction rate of FTS depends on kinetics and thermodynamics factors. As the temperature increases over 300 °C, the rate of the RWGS reaction (CO formation) may be faster than the FTS (CO consumption) rate, leading to a CO conversion decrease at the temperature region of 300∼340 °C (Figure 6a).

Figure 6b shows the selectivity of the hydrocarbon products measured as a function of the temperature over the Fe/Cu/Al/K catalyst from the model bio-oil-syngas. With an increase in the temperature from 240 to 340 °C, it was observed that the desired C_{5+} selectivity in hydrocarbon products smoothly decreased from 56.3% to 40.5%. At the same time, CH_4 and C_2-C_4 selectivity increase gradually with an increase in the temperature. Generally, the FT reaction produces hydrocarbons of variable chain lengths. Selectivity of the hydrocarbons (product distribution) is influenced by a number of factors, either catalyst-dependent [type of metal (iron or cobalt), support, preparation, preconditioning, and age of the catalyst] or noncatalyst-dependent (composition of the feed gas, temperature, pressure, W/F, and reactor type).[64] A high liquid selectivity (C_{5+} selectivity) is necessary to obtain a maximum amount of long hydrocarbon chains. FTS is kinetically controlled, and the intrinsic kinetics consist of stepwise chain growth on the catalyst surface. FTS product selectivity is determined by the ability of a catalyst to catalyze chain-propagation versus chain-termination reactions. Irrespective of the catalyst type or the feed gas composition, it is always found that the CH_4 selectivity increases as the temperature increases; that is, the probability of chain growth decreases.[50] With regard to the hydrocarbon distribution observed, it is reasonable that selectivity toward the CH_4 and C_2-C_4 fraction increased with increasing temperature, whereas selectivity to C_{5+} decreased, because the Fischer−Tropsch polymerization reaction is an exothermic reaction and an increase of the reaction temperature always shifts the hydrocarbon products toward shorter-chain hydrocarbons. The overall effect is in line with thermodynamic expectations, namely, that shorter chain hydrocarbons are much more favored than higher ones at high temperatures in Fischer−Tropsch synthesis. On the other hand, the selectivity of olefins in C_2-C_4 hydrocarbons reached about 75∼79%, and no significant change with an increase in temperature was found in the investigated temperature range. The olefin content in the hydrocarbon products reflects secondary olefin reactions such as reinsertion into the

(62) Spath, P. L.; Dayton, D. C. Preliminary Screening − Technical and Economic Assessment of Synthesis Gas to Fuels and Chemicals with Emphasis on the Potential for Biomass-Derived Syngas. NREL/TP-510-34929; National Renewable Energy Laboratory: Golden, CO; pp 94.

(63) Niemelä, M.; Nokkosmäki, M. *Catal. Today* **2005**, *100*, 269−274.

(64) Tijmensen, M. J. A.; Faaij, A. P. C.; Hamelinck, C. N.; Hardeveld, M. R. M. *Biomass Bioenergy* **2002**, *23*, 129−152.

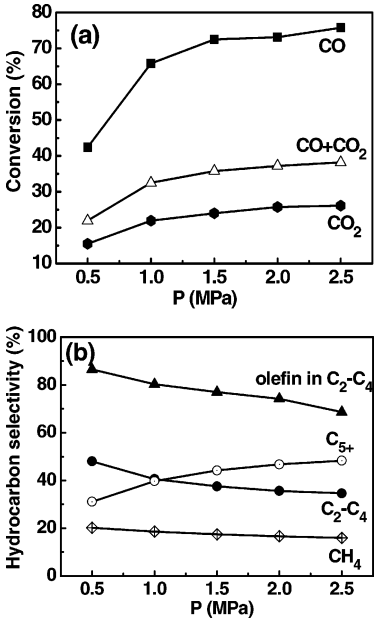

Figure 7. (a) Effect of pressure on CO conversion, CO_2 conversion, and total carbon ($CO + CO_2$) conversion. (b) Effect of pressure on the selectivity of hydrocarbon products. Model bio-oil-syngas: $H_2/CO/CO_2/N_2$ (vol %) = 62:8:25:5. Reaction conditions: $T = 300$ °C and $W/F = 12.5$ g_{cat}·h·mol^{-1}.

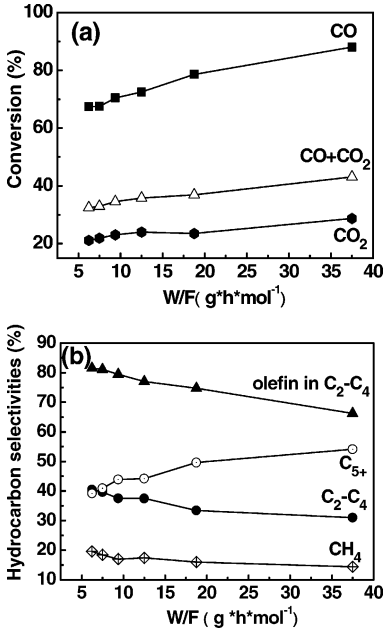

Figure 8. (a) Effect of W/F on CO conversion, CO_2 conversion, and total carbon ($CO + CO_2$) conversion. (b) Effect of W/F on the selectivity of hydrocarbon products. Model bio-oil-syngas: $H_2/CO/CO_2/N_2$ (vol %) = 62:8:25:5. Reaction conditions: $T = 300$ °C and $P = 1.5$ MPa.

chain-growth process, hydrogenation, and hydrogenolysis in addition to the primary olefin selectivity. It is indicated that the potassium-promoted iron catalyst has a very low propensity for olefin secondary reactions allowing for the production of linear terminal olefins even at elevated temperatures.

3.2.3. Effect of Pressure on the FTS Reaction. It was also observed that the total pressure prominently affected the FTS activity and the hydrocarbon products distribution. Figure 7 shows the effect of pressure on the CO conversion, CO_2 conversion, total carbon ($CO + CO_2$) conversion, and the selectivity of the hydrocarbon products using the bio-oil-syngas at 300 °C and a W/F of 12.5 g_{cat}·h·mol^{-1}. With an increase in the reaction pressure from 0.5 to 1.5 MPa, the CO conversion remarkably increases from 42.4% to 72.5%. When the pressure is further increased from 1.5 to 2.5 MPa, the CO conversion slightly changes from 72.5% to about 75.8%. It is well-known that the FTS reaction has positive pressure-dependence since the number of product molecules is less than the number of reactant molecules. Therefore, it is reasonable that an increase of reaction pressure would promote the FTS reaction, which consequently leads to an increase in the CO conversion.

With an increase in the pressure from 0.5 to 2.5 MPa (Figure 7a), it was also observed that the CO_2 conversion increased from 15.5% to 26.1%, and the ($CO + CO_2$) conversion increased from 21.9% to 38.2%. Generally, pressure has no effect on CO_2 conversion by the reverse water−gas shift reaction (reaction 4) according to chemical equilibrium theory, because the number of molecules on the reactant side is the same as that on the product side. For CO_2 hydrogenation to hydrocarbon over the iron-based catalyst Fe/Cu/Al/K, however, it would be considered a two-step mechanism: namely, partial reduction of CO_2 to CO by the reverse water−gas shift reaction (reaction 4) and subsequent Fischer−Tropsch synthesis (reactions 5−7). The promotion of the FTS reactions caused by an increase in pressure would consume more CO. This, in turn, would cause a shift of equilibrium toward the reverse water−gas shift reaction direction, leading to an increase in CO_2 conversion. Furthermore, it was found that the pressure has a significant effect on the reaction performance only in the low-pressure range, which favors reducing the compression cost of the bio-oil-syngas feed.

On the other hand, the reaction pressure also affects the distribution of the hydrocarbon products, as shown in Figure 7b. It was found that the selectivity of the long-chain hydrocarbons (C_{5+}) increases with increasing pressure, while the selectivity of CH_4 and C_2-C_4 appeared to be an adverse trend. The selectivity of olefin in C_2-C_4 products also decreases from 86.5% to 68.6% when the total pressure increases from 0.5 to 2.5 MPa. It is implied that an increase of pressure within an appropriate range (1.0∼2.0 MPa) is beneficial to inhibiting short-chain hydrocarbon (C_1-C_4) formation and increasing the selectivity of desired long-chain hydrocarbons (C_{5+}).

3.2.4. Effect of Contact Time (W/F) on the FTS Reaction. The contact time, described by W/F (W is the weight of the catalyst; F is the molar flow rate of the model syngas), is another important factor affecting the FTS reaction. In this work, the effect of W/F on the CO conversion, the CO_2 conversion, the total carbon ($CO + CO_2$) conversion, and the selectivity of the hydrocarbon products has been investigated for $W/F = 6.25 \sim 37.5$ g_{cat}·h·mol^{-1}, $T = 300$ °C, and $P = 1.5$ MPa with the model bio-oil-syngas (Figure 8). The CO and CO_2 conversion increases as W/F increases, because the adsorption and the residence time of the reactants on the surface of the catalyst increase with an increase in W/F. As can be seen in Figure 8a, the CO conversion increases from 67.4% to 88.0%, and the CO_2 conversion increases from 21.1% to 28.7% as W/F increases from 6.25 to 37.5 g_{cat}·h·mol^{-1}. The total carbon conversion of ($CO + CO_2$) displays an increasing trend that is similar to those of CO and CO_2 with increasing W/F. Figure 8b presents the selectivity of hydrocarbon products measured as a function of W/F. It was found that the selectivity of the long-chain hydrocarbons (C_{5+}) significantly increases from 39.2% to 54.1% with increasing W/F. However, the selectivities of CH_4 and C_2-C_4 and olefin selectivity in C_2-C_4 decrease as W/F increases. The above results indicate that a higher W/F enhances the production of the heavier fractions of the hydrocarbons. Increasing W/F would increase the adsorbed amount of C atoms as well as H atoms

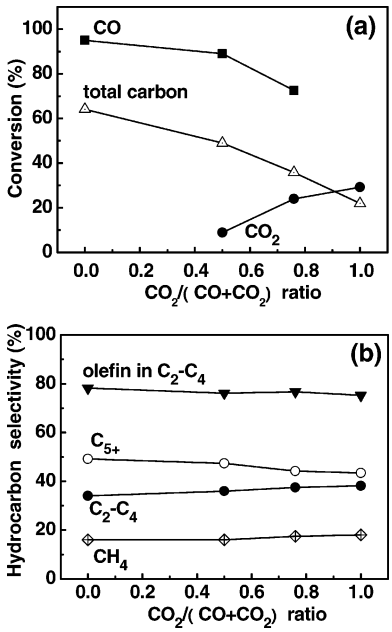

Figure 9. (a) Effect of $CO_2/(CO + CO_2)$ ratio of the syngas on CO conversion, CO_2 conversion, and total carbon conversion. (b) Effect of $CO_2/(CO + CO_2)$ ratio of the syngas on the selectivity of hydrocarbon products. Reaction conditions: $T = 300$ °C, $P = 1.5$ MPa, and $W/F = 12.5$ g_{cat}·h·mol^{-1}.

and prolong the residence time of the reactants or intermediates on the catalyst surface. The longer residence time may be favorable to the secondary reactions of the formed intermediate products through further hydrogenation and oligomerization, causing an increase in the selectivity of the long-chain hydrocarbons (e.g., C_{5+}).

3.2.5. Effect of $CO_2/(CO+CO_2)$ Ratio on the FTS Reaction. Generally, the syngas derived from bio-oil via catalytic steam reforming is a CO_2-rich syngas. The volume ratio of $H_2/CO/CO_2$ in the syngas mainly depends on the types of reforming catalyst, reforming temperature, S/C ratio, and so forth (see Tables 3 and 4). In addition, the composition of bio-oil-syngas can be adjusted by a combination of methane reforming, the RWGS reaction, and CO_2 removal before entering into the synthesis loop. The $CO_2/(CO + CO_2)$ ratio will be variable depending on the reforming conditions and the method of combination. In this work, we investigated the FTS reaction by varying the $CO_2/(CO + CO_2)$ ratio of the syngas at $T = 300$ °C, $P = 1.5$ MPa, $H_2/(CO + CO_2) = 1.87$, and $W/F = 12.5$ g_{cat}·h·mol^{-1}. The dependence of the catalytic activity of the Fe/Cu/Al/K catalyst on the feed gas composition is illustrated in Figure 9a. For the syngas of H_2/CO (i.e., $r = 0$), the CO conversion reached about 95%, and a highest total carbon conversion of about 64.1% was obtained. It should be pointed out that 30.9% of the total carbon converted to CO_2 via the water−gas shift reaction over the Fe/Cu/Al/K catalyst when H_2/CO ($r = 0$) was used as syngas. With an increase of the r value to 0.5, CO conversion slightly decreases to 89% and CO_2 conversion remains very low (<9%). The above results indicate that CO hydrogenation is the preferred reaction up to an r value of 0.5. When the r value is further increased to 0.76, CO conversion smoothly decreases to 72.5%. On the other hand, CO_2 conversion increases from 8.9% to 29.2% with an increase in r from 0.5 to 1. When H_2/CO_2 ($r = 1$) is used as syngas, according to the two-step mechanism, CO is produced as an intermediate via the RWGS reaction. It was found that 7.3% of the total carbon in H_2/CO_2 converts to CO in the effluent from the FT reactor. The total carbon conversion smoothly decreases from 64.1% (H_2/CO as syngas) to 21.9% (H_2/CO_2 as syngas) in the investigated range. The result indicates that the rate of CO_2 hydrogenation is about 3 times lower than that of CO hydrogenation. For the FT synthesis over an iron catalyst, the active phase is believed to be the iron carbide species, while the contribution of other phases such as metallic iron has not been clarified. When H_2/CO is used as syngas, active carbide species are formed on the catalyst surface as well as on the metallic iron during the reaction with CO. For CO_2 hydrogenation, CO_2 converts to CO via the RWGS reaction, and then CO reacts with hydrogen to produce hydrocarbons. In the presence of CO_2, a greater amount of water is produced than with CO hydrogenation. It is well-known that CO_2 and water can oxidize active carbide species of the iron catalyst and result in only a slight quantity of carbide species formed.[65] In other words, with the increase of CO_2 partial pressure in the syngas, the concentration of the active carbide species on the catalyst surface gradually decreases, and the lower concentration of active carbide species results in a lower conversion efficiency of CO_2.

Figure 9b presents the effect of the $CO_2/(CO + CO_2)$ ratio (r) on the hydrocarbon products' selectivity and olefin selectivity in C_2-C_4 hydrocarbons. It was found that there is no prominent influence of the r value on hydrocarbon products' selectivity. Only a slight increase in CH_4 selectivity and C_2-C_4 selectivity was found with an increase in the r value in our investigated range. On the contrary, the desired C_{5+} selectivity slightly decreases from 49.2% to 43.4% when the r value increases from 0 to 1. It also can be seen that olefin selectivity in C_2-C_4 was nearly identical, independent of the syngas composition. This shows that neither methane formation nor chain growth is controlled by the partial pressure of CO with potassium-promoted iron catalysts, which agreed with the previous observation.[66]

Finally, it should be pointed out that one of the most important advantages to generating syngas from bio-oil via catalytic steam reforming is that one can obtain very high hydrogen yields and hydrogen concentrations in the bio-oil-syngas produced versus those with biomass gasification. For example, a hydrogen yield as high as about 71% over the C12A7/15%Mg catalyst was obtained, and the maximum carbon conversion reached over 93% under steam reforming conditions ($T = 750$ °C, S/C = 6.0, and GHSV = 26 000 h^{-1}). CO_2-rich characteristics of the bio-oil-syngas will lead to lower use efficiency of the carbon than that of conventional syngas (H_2/CO). As can be seen from Figure 9, CO hydrogenation was the primary reaction as $r < 0.5$, and CO_2 conversion plays a more important role in total carbon conversion with an increase of r in the range of $r > 0.5$. It was also found that the reaction rate with H_2/CO_2 syngas over Fe/Cu/Al/K is about 2−4 times lower than that with H_2/CO hydrogenation. So, CO_2-rich characteristics of the bio-oil-syngas will lead to a lower use efficiency of carbon than that of conventional syngas (H_2/CO). To further improve the efficiency of the FTS process using bio-oil-syngas, enhancement of the conversion of CO_2 to CO via the RWGS reaction and/or adjustment of the composition of bio-oil-syngas by the combination of methane reforming and CO_2 removal and so forth still needs to occur. In order to improve the economy of bio-oil to clean liquid biofuel, the large hydrocarbons (C_{5+}) can be hydrocracked to form gasoline or diesel of excellent quality,

(65) Ando, H.; Matsumura, Y.; Souma, Y. *J. Mol. Catal. A: Chem.* **2000**, *154*, 23−29.

(66) Riedel, T.; Claeys, M.; Schulz, H.; Schaub, G.; Nam, S. S.; Jun, K. W.; Choi, M. J.; Kishan, G.; Lee, K. W. *Appl. Catal., A* **1999**, *186*, 201−213.

and a fraction of short hydrocarbons is used in a combined cycle (using a gas turbine for bioenergy generation) with the remainder of the syngas.

4. Conclusions

The present results show that FTS using the bio-oil-syngas, produced by the steam reforming of bio-oil, would be a promising option to directly synthesize clean liquid biofuels. The characteristics of the bio-oil-syngas generated via the catalytic steam reforming of the homemade bio-oil and the FTS performance using the model bio-oil-syngas have been studied, which can be summarized as below.

The bio-oil-syngas produced was a CO_2-rich syngas, in which H_2 and CO_2 were the major reforming products of the bio-oil together with a small amount of CO and CH_4 in the effluent gaseous products. The performance of catalytic steam reforming of bio-oil mainly depends on the reforming temperature (T), the ratio of molar steam to molar carbon fed (S/C), and the reforming catalysts. The hydrogen yield and the carbon conversion in the reforming process of the bio-oil increased with increasing temperature and S/C ratio. The Pt-based catalyst (1%Pt/γ-Al_2O_3) shows the best performance among our tested catalysts (C12A7/15%Mg, 12%Ni/γ-Al_2O_3, and 1%Pt/γ-Al_2O_3). However, such catalysts may be not practical due to their high cost. The C12A7/15%Mg catalyst also shows good reforming activity for producing the bio-oil-syngas, giving a highest hydrogen yield near 71% and a maximum carbon conversion at about 93% under steam reforming conditions of T = 750 °C, S/C = 6.0, and GHSV = 26 000 h^{-1}. The composition of the bio-oil-syngas using the C12A7/15%Mg catalyst includes about 62% H_2, 25% CO_2, 8% CO, and 5% CH_4 at T = 750 °C, S/C = 6.0, and GHSV = 26 000 h^{-1}.

It was found that the coprecipitated Fe/Cu/Al/K catalyst has good FTS performance both for CO hydrogenation and simultaneously for CO_2 hydrogenation. The optimum content ratio of Fe/Cu/Al/K for FTS using bio-oil-syngas is about 100:6:16:6 (wt ratio). The composition and main physical and chemical properties of the Fe/Cu/Al/K catalyst have been investigated by characterizations. It is considered that the Fe/Cu/Al/K catalyst is one of the most promising candidates for direct synthesis of the liquid bio-fuel using the bio-oil-syngas.

The key factors which influence the FTS performance using the bio-oil-syngas over the Fe/Cu/Al/K catalyst are reaction temperature, pressure, contact time (W/F), and composition of the bio-oil-syngas. Relatively higher pressure and longer contact time with a suitable temperature are favorable to obtain a higher carbon conversion (i.e., conversion of CO, CO_2, and total carbon) and higher selectivity of C_{5+}. It was found that the optimum conditions over the Fe/Cu/Al/K catalyst are T = 280∼300 °C, P = 1.0∼2.0 MPa, and W/F > 12.5 g_{cat}·h·mol^{-1}, in our investigated range. A CO conversion of 72.5% and a CO_2 conversion of 24% with a C_{5+} selectivity of 44.2% were obtained under typical reaction conditions of T = 300 °C, P = 1.5 MPa, and W/F = 12.5 g_{cat}·h·mol^{-1} with a syngas of H_2/CO/CO_2 = 62:8:25. It was also found that the CO_2/(CO + CO_2) ratio of the syngas has a remarkable effect on FTS performance and r < 0.5 is more suitable for FTS in our investigated range. For CO_2 hydrogenation, a two-step process would be considered: the first step is the conversion of CO_2 to CO via the reverse water−gas shift reaction, and the subsequent step involves the hydrogenation of CO to produce hydrocarbons with CO as the intermediate. The efficiency of CO_2 hydrogenation over the Fe/Cu/Al/K catalyst is about 2∼4 times lower than that of CO hydrogenation. To further promote FTS via bio-oil-syngas, it seems necessary to decrease the CO_2 content in the bio-oil-syngas through a combination of methane co-reforming, CO_2 removal, and enhancement of the reverse water−gas shift reaction.

Acknowledgment. The authors thank Prof. Yilu Fu and Prof. Peiyan Lin for their helpful discussion. Q.X.L. thanks the support of the "863 Program (2006AA05Z118)" by the Ministry of Science and Technology of the People's Republic of China and the "BRP Program 2002" by the Chinese Academy of Science.

EF0700275